12th International Conference on Domain Decomposition Methods
Editors: Tony Chan, Takashi Kako, Hideo Kawarada, Olivier Pironneau,

33. Domain decomposition methods for a coupled vibration between an acoustic field and a plate

Xiaobing Feng[1], Zhenghui Xie[2]

Introduction

The coupled vibration between an acoustic field and a plate is encountered in many engineering and industrial applications. The interaction between the wind and a windshield of a car is an interesting example found in the automobile industry. Mathematically, such an interaction is described by the coupled system of the second order scalar wave equation and the fourth order plate vibration equation. Since the thickness of the plate is negligible, the plate serves a dual role in the model. It is the solid medium and in the same time it is the interface between the acoustic field and the solid (so it is a part of the boundary of the acoustic field), where they interact each other.

Let $\Omega \subset R^3$ be a three-dimensional acoustic field and $\Gamma_0 \subset R^2$, a part of the boundary $\partial\Omega$, denote the domain of the plate. Let $\Gamma_1 = \partial\Omega \backslash \Gamma_0$ be the remaining portion of the boundary of Ω. Let $p = p(x_1, x_2, x_3)$ denote the pressure function of the fluid in the acoustic field Ω and $u = u(x')$ ($x' = (x_1, x_2)^t$) denote the vertical displacement of the plate Γ_0. Then the governing partial differential equations of the fluid–plate interaction is given by [CS76]

$$\frac{1}{c^2} p_{tt} - \Delta p = f, \qquad \text{in } \Omega \times (0,T), \tag{1}$$

$$\frac{1}{c} p_t + \frac{\partial p}{\partial n} = 0, \qquad \text{on } \Gamma_1 \times (0,T), \tag{2}$$

$$\frac{\partial p}{\partial n} + \rho_f u_{tt} = 0, \qquad \text{on } \Gamma_0 \times (0,T), \tag{3}$$

$$\rho_s u_{tt} + D\Delta_{\Gamma_0}^2 u = p, \qquad \text{on } \Gamma_0 \times (0,T), \tag{4}$$

$$u = \frac{\partial u}{\partial \nu} = 0, \qquad \text{on } \partial\Gamma_0 \times (0,T), \tag{5}$$

$$p(x,0) = p_0(x), \quad p_t(x,0) = p_1(x), \qquad \text{in } \Omega, \tag{6}$$

$$u(x',0) = u_0(x'), \quad u_t(x',0) = u_1(x'), \qquad \text{on } \Gamma_0, \tag{7}$$

where c is the sound speed in the fluid, D flexural rigidity of plate. ρ_f and ρ_s are the air mass density and plate mass density, and n and ν are the outward normal vector on Γ_0 and $\partial\Gamma_0$, respectively. $\Delta_{\Gamma_0}^2$ stands for the biharmonic operator defined on Γ_0 in variables x_1, x_2.

In the model, equations (3) and (4) are the interface condition which describe the interaction between the acoustic field and the plate. Equation (2) is the first order absorbing boundary condition for the acoustic wave. We use this boundary condition,

[1]Department of Mathematics, The University of Tennessee, Knoxville, TN 37996, U.S.A. xfeng@math.utk.edu
[2]LASG, Institute of Atmospheric Physics, Chinese Academy of Sciences, Beijing 100080, China. xzh@lasgsgi4.iap.ac.cn

instead of the Dirichlet condition as used in [CS76], to limit the (computational) size of the acoustic domain. Using the energy method it is not hard to show the following theorem.

Theorem 1 *For $f \in H^{-1}(\Omega)$, $p_j \in H^{1-j}(\Omega)$, and $u_j \in H^{2-j}(\Gamma_0)$, $j = 0, 1$, the problem (1)–(7) has a unique solution $(p, u) \in L^2(H^1(\Omega)) \cap H^1(L^2(\Omega)) \times L^2(H^2(\Gamma_0)) \cap H^1(H^1(\Gamma_0))$.*

The goal of this paper is to develop some parallelizable non–overlapping domain decomposition iterative methods for effectively solving the problem (1)–(7). Due to the heterogeneous nature of the problem, the non–overlapping domain decomposition approach is a very practical and natural way to solve the problem. In §2 we introduce two classes of domain decomposition iterative methods to decouple the problem into fluid and plate subdomain problems. In §3 we establish usefulness of these methods by showing their strong convergence in the energy norm of the underlying problem. Finally, in §4 we present some numerical models based on finite difference methods, and some numerical tests to validate the theory and to show effectiveness of the methods, in particular, with respect to different choices of the relaxation parameter.

Domain decomposition methods

In this section we first propose a family of new interface conditions which are equivalent to the original interface condition (3). This is the key step towards developing non-overlapping domain decomposition methods for the problem. Based on these new interface conditions, we then introduce two classes of parallelizable non-overlapping domain decomposition iterative algorithms for solving the system (1)–(7) and show their strong convergence in the energy norm of the underlying interaction problem. The methods and the analysis of this paper are inspired by its companion paper [Fen98], where non-overlapping domain decomposition methods were developed for a general fluid–solid interaction problem in which the solid is a 3–dimensional elastic body. For applications of domain decomposition methods to other heterogeneous problem, we refer to [CF99, Fen98, QPV92] and references therein.

To decouple the problem on the interface, we rewrite the interface condition (3) as

$$\frac{\partial p}{\partial n} + \alpha p_t = -\rho_f u_{tt} + \alpha p_t, \qquad \text{on } \Gamma_0 \times (0, T), \tag{8}$$

for any nonzero constant α.

Hence, the problem (1)–(7) is equivalent to the problem consisting equations (1), (2), (8), and (4)–(7). That is,

$$\frac{1}{c^2}p_{tt} - \Delta p = f, \qquad \text{in } \Omega \times (0,T), \tag{9}$$
$$\frac{1}{c}p_t + \frac{\partial p}{\partial n} = 0, \qquad \text{on } \Gamma_1 \times (0,T), \tag{10}$$
$$\frac{\partial p}{\partial n} + \alpha p_t = -\rho_f u_{tt} + \alpha p_t, \qquad \text{on } \Gamma_0 \times (0,T), \tag{11}$$
$$\rho_s u_{tt} + D\Delta^2_{\Gamma_0} u = p, \qquad \text{on } \Gamma_0 \times (0,T), \tag{12}$$
$$u = \frac{\partial u}{\partial \nu} = 0, \qquad \text{on } \partial\Gamma_0 \times (0,T), \tag{13}$$
$$p(x,0) = p_0(x), \quad p_t(x,0) = p_1(x), \qquad \text{in } \Omega, \tag{14}$$
$$u(x',0) = u_0(x'), \quad u_t(x',0) = u_1(x'), \qquad \text{on } \Gamma_0. \tag{15}$$

Domain decomposition algorithms

Based on the above new form of the interface conditions we propose the following two types of iterative algorithms. The first one resembles to block Gauss-Seidel iteration and the other resembles block Jacobi iteration.

Algorithm 1

Step 1: $\forall p^0 \in H^1(L^2(\Gamma_0))$.

Step 2: Compute $\{(u^k, p^k)\}_{k\geq 1}$ by solving

$$\rho_s u^k_{tt} + D\Delta^2_{\Gamma_0} u^k = p^{k-1}, \qquad \text{on } \Gamma_0 \times (0,T), \tag{16}$$
$$u^k = \frac{\partial u^k}{\partial \nu} = 0, \qquad \text{on } \partial\Gamma_0 \times (0,T), \tag{17}$$
$$u^k(x',0) = u_0(x'), \quad u^k_t(x',0) = u_1(x'), \qquad \text{on } \Gamma_0 \times (0,T); \tag{18}$$
$$\frac{1}{c^2}p^k_{tt} - \Delta p^k = f, \qquad \text{in } \Omega \times (0,T), \tag{19}$$
$$\frac{\partial p^k}{\partial n} + \alpha p^k_t = -\rho_f u^k_{tt} + \alpha p^{k-1}_t, \qquad \text{on } \Gamma_0 \times (0,T), \tag{20}$$
$$\frac{\partial p^k}{\partial n} + \frac{1}{c}p^k_t = 0, \qquad \text{on } \Gamma_1 \times (0,T), \tag{21}$$
$$p^k(x,0) = p^k_0(x), \quad p^k_t(x,0) = p_1(x), \qquad \text{in } \Omega. \tag{22}$$

Algorithm 2

Step 1: $\forall H^2(L^2(\Gamma_0)) \times H^1(L^2(\Gamma_0))$.

Step 2: Compute $\{(u^k, p^k)\}_{k\geq 1}$ by solving

$$\rho_s u^k_{tt} + D\Delta^2_{\Gamma_0} u^k = p^{k-1}, \qquad \text{on } \Gamma_0 \times (0,T), \tag{23}$$
$$u^k = \frac{\partial u^k}{\partial \nu} = 0, \qquad \text{on } \Gamma_0 \times (0,T), \tag{24}$$
$$u^k(x',0) = u_0(x'), \quad u^k_t(x',0) = u_1(x'), \qquad \text{on } \Gamma_0 \times (0,T); \tag{25}$$
$$\frac{1}{c^2}p^k_{tt} - \Delta p^k = f, \qquad \text{in } \Omega \times (0,T), \tag{26}$$
$$\frac{\partial p^k}{\partial n} + \alpha p^k_t = -\rho_f u^{k-1}_{tt} + \alpha p^{k-1}_t, \qquad \text{on } \Gamma_0 \times (0,T), \tag{27}$$
$$\frac{\partial p^k}{\partial n} + \frac{1}{c}p^k_t = 0, \qquad \text{on } \Gamma_1 \times (0,T), \tag{28}$$
$$p^k(x,0) = p_0(x), \quad p^k_t(x,0) = p_1(x), \qquad \text{in } \Omega. \tag{29}$$

Convergence analysis

In this subsection we shall establish the utility of Algorithm 1 and 2 by showing their strong convergence. Since the proof of the convergence of Algorithm 1 and 2 are similar, we only give the proof for Algorithm 1.

Define the error functions $e^k = p - p^k, r^k = u - u^k$. It follows from (1)–(7) and (9)–(15) that

$$\rho_s r^k_{tt} + D\Delta^2_{\Gamma_0} r^k = e^{k-1}, \qquad \text{on } \Gamma_0 \times (0,T), \tag{30}$$

$$r^k = \tfrac{\partial r^k}{\partial \nu} = 0, \qquad \text{on } \Gamma_0 \times (0,T), \tag{31}$$

$$r^k(x',0) = r^k_t(x',0) = 0, \qquad \text{in } \Omega \times (0,T); \tag{32}$$

$$\tfrac{1}{c^2} e^k_{tt} - \Delta e^k = 0, \qquad \text{in } \Omega \times (0,T), \tag{33}$$

$$\tfrac{\partial e^k}{\partial n} + \alpha e^k_t = -\rho_f r^k_{tt} + \alpha e^{k-1}_t, \qquad \text{on } \Gamma_0 \times (0,T), \tag{34}$$

$$\tfrac{\partial e^k}{\partial n} + \tfrac{1}{c} e^k_t = 0, \qquad \text{on } \Gamma_1 \times (0,T), \tag{35}$$

$$e^k(x,0) = e^k_t(x,0) = 0, \qquad \text{in } \Omega. \tag{36}$$

Lemma 1 *For $\forall \tau \in (0,T]$, we have*

$$\int_0^\tau \int_{\Gamma_0} e^{k-1}_t r^k_{tt} ds dt = \tfrac{1}{2}[\|\sqrt{\rho_s} r^k_{tt}(\cdot,\tau)\|^2_{0,\Gamma_0} + \|\sqrt{D}\Delta_{\Gamma_0} r^k_t(\cdot,\tau)\|^2_{0,\Gamma_0}]. \tag{37}$$

$$\int_0^\tau \int_{\Gamma_0} \tfrac{\partial e^k}{\partial n} e^k_t ds dt = \tfrac{1}{2}\left[\left\|\tfrac{1}{c} e^k_t(\cdot,\tau)\right\|^2_{0,\Omega} + \|\nabla e^k(\cdot,\tau)\|^2_{0,\Omega}\right] + \int_0^\tau \left\|\tfrac{1}{\sqrt{c}} e^k_t(\cdot,t)\right\|^2_{0,\Gamma_1} dt \tag{38}$$

Proof: Testing (30)) against r^k_{tt} after taking one derivative with respect to t, we get

$$\int_{\Gamma_0} e^{k-1}_t r^k_{tt} ds dt = \frac{1}{2}\frac{d}{dt}\|\sqrt{\rho_s} r^k_{tt}\|^2_{0,\Gamma_0} + \frac{1}{2}\frac{d}{dt}\left\|\sqrt{D}\Delta_{\Gamma_0} r^k_t\right\|^2_{0,\Gamma_0}. \tag{39}$$

Integrating (39) in t from 0 to τ yields (37).

Similarly, test (33) against e^k_t, we get

$$\int_{\Gamma_0} \frac{\partial e^k}{\partial n} e^k_t ds = \frac{1}{2}\frac{d}{dt}\left[\left\|\frac{1}{c} e^k_t\right\|^2_{0,\Omega} + \left\|\nabla e^k\right\|^2_{0,\Omega}\right] + \left\|\frac{1}{\sqrt{c}} e^k_t\right\|^2_{0,\Gamma_1}. \tag{40}$$

Integrating (40) in t from 0 to τ gives (38).

Notice that in the proof we have used the fact that

$$r^k(\cdot,0) = r^k_t(\cdot,0) = r^k_{tt}(\cdot,0) = \Delta_{\Gamma_0} r^k(\cdot,0) = e^k_t(\cdot,0) = e^k(\cdot,0) = 0,\ \nabla e^k(\cdot,0) = 0.$$

Next, define the "pseudo-energy"

$$E_k(\tau) \equiv \left\|\frac{\partial e^k}{\partial n} + \alpha e^k_t\right\|^2_{L^2((0,\tau),L^2(\Gamma_0))} = \int_0^\tau \int_{\Gamma_0} \left[\frac{\partial e^k}{\partial n} + \alpha e^k_t\right]^2 ds dt. \tag{41}$$

By a direct calculation, we can show that $\{E_k(\tau)\}$ satisfy the following identity.

Lemma 2 *For $k \geq 1$ there holds the following identity*

$$E_k(\tau) = E_{k-1}(\tau) - R_{k-1}(\tau), \tag{42}$$

where

$$\begin{aligned} R_{k-1}(\tau) &= \left\| \frac{\partial e^{k-1}}{\partial n} \right\|^2_{L^2((0,\tau),L^2\Gamma_0))} - \rho_f^2 \|r_{tt}^k\|^2_{L^2((0,\tau),L^2(\Gamma_0))} \\ &\quad + 2\alpha \int_0^\tau \int_{\Gamma_0} \frac{\partial e^{k-1}}{\partial n} e_t^{k-1} ds dt + 2\alpha\rho_f \int_0^\tau \int_{\Gamma_0} e_t^{k-1} r_{tt}^k ds dt. \end{aligned} \tag{43}$$

An immediate consequence of Lemma 1 is the following lemma.

Lemma 3 *For $k \geq 1$ there holds the equality*

$$\begin{aligned} R_{k-1}(\tau) &= [\alpha\rho_f \|\sqrt{\rho_s} r_{tt}^k(\cdot,\tau)\|^2_{0,\Gamma_0} - \rho_f^2 \|r_{tt}^k\|^2_{L^2((0,\tau);L^2(\Gamma_0))}] \\ &\quad + \alpha \left[\rho_f \|\sqrt{D}\Delta_{\Gamma_0} r_t^k(\cdot,\tau)\|^2_{0,\Gamma_0} + \left\| \frac{1}{c} e_t^k(\cdot,\tau) \right\|^2_{0,\Omega} + \|\nabla e^k(\cdot,\tau)\|^2_{0,\Omega} \right] \\ &\quad + \left\| \frac{\partial e^{k-1}}{\partial n} \right\|^2_{L^2((0,\tau);L^2(\Gamma_0))} + \alpha \int_0^\tau \left\| \frac{1}{\sqrt{c}} e_t^k(\cdot,t) \right\|^2_{0,\Gamma_1} dt. \end{aligned} \tag{44}$$

Theorem 2 *If $\alpha > T\rho_f/\rho_s$, then*

(1) $p^k \to p$ strongly in $L^2((0,T);H^1(\Omega)) \cap H^1((0,T);L^2(\Omega))$.
(2) $u^k \to u$ strongly in $H^1((0,T);H^2(\Gamma_0)) \cap H^2((0,T);L^2(\Gamma_0))$.

Proof: It is easy to check that (42) implies that

$$\int_0^T E_k(\tau) d\tau = \int_0^T E_0(\tau) d\tau - \sum_{l=0}^{k-1} \int_0^T R_l(\tau) d\tau. \tag{45}$$

Since

$$\int_0^T \|r_{tt}^k\|^2_{L^2((0,\tau);L^2(\Gamma_0))} d\tau = \int_0^T \left(\int_0^\tau \|r_{tt}^k(\cdot,t)\|^2_{0,\Gamma_0} dt \right) d\tau \leq T \|r_{tt}^k\|^2_{L^2((0,T);L^2(\Gamma_0))}, \tag{46}$$

we have

$$\begin{aligned} &\int_0^T \left[\alpha\rho_f \|\sqrt{\rho_s} r_{tt}^k(\cdot,\tau)\|^2_{0,\Gamma_0} - \rho_f^2 \|r_{tt}^k\|^2_{L^2((0,\tau);L^2(\Gamma_0))} \right] d\tau \\ &\qquad \geq \rho_f(\alpha\rho_s - T\rho_f) \|r_{tt}^k\|^2_{L^2((0,T);L^2(\Gamma_0))}. \end{aligned} \tag{47}$$

Hence, if $\alpha > T\rho_f/\rho_s$, every term on the right hand side of (43) is a nonnegative term. Now it follows from (45) that

$$\sum_{l=0}^{\infty} \int_0^T R_l(\tau) d\tau < \infty,$$

which implies that

$$\lim_{l\to\infty} \int_0^T R_l(\tau)d\tau = 0. \tag{48}$$

Finally, the proof is completed by combining (44), (47) and (48).

Numerical experiments

We shall present some numerical tests for the domain decomposition algorithms developed in the previous sections. Finite difference methods are used to discretize the differential equations. The acoustic field is chosen as the unit cubic $\Omega = [0,1]^3$ and the plate domain is the unit square $\Gamma_0 = [0,1]^2$ on the x_1x_2- plane. Zero source function $f \equiv 0$ and the parameters $c = 2.5, D = 2, \rho_f = 5, \rho_s = 50$ are assumed in all tests. Also, the uniform meshes are used in both acoustic domain and the plate domain. The mesh size of the acoustic domain is $\Delta x_1 = \Delta x_2 = \Delta x_3 = 0.1$ and the mesh size of the the plate domain is $\Delta x_1 = \Delta x_2 = 0.05$. The time step size $\Delta t = 0.01$ is used in all tests. Finally, we choose the following initial conditions.

$$p_0(x) = 1, \quad p_1(x) = 0.1, \quad u_0(x_1, x_2) = \sin \pi x_1 \sin \pi x_2, \quad u_1(x_1, x_2) = 0.1.$$

Figure 1 shows the plate displacement (u) profiles at four different time steps, in which (a)–(d) are plots of u at $t = 4\Delta t, 8\Delta t, 12\Delta t, 16\Delta t$, respectively. Figure 2 gives the pressure (p) profiles on the interface $x_3 = 0$ at (a) $t = 4\Delta t$, (b) $t = 8\Delta t$, (c) $t = 12\Delta t$, (d) $t = 16\Delta t$, which show the acoustic wave action on the plate. Figure 3 shows the contour plots of the pressure p on the cross section of Ω at $x_1 = 0.5$ at (a) $t = 4\Delta t$, (b) $t = 8\Delta t$, (c) $t = 12\Delta t$, (d) $t = 16\Delta t$. Figure 4 presents a comparison of the iteration numbers for different choices of the relaxation parameter α at various time steps. Graph (a) compares the iteration numbers for $\alpha = 10^{-9}$ and $\alpha = 10$, while Graph (b) compares for $\alpha = 1$ and $\alpha = 100$. The criterion used to stop the domain decomposition iteration at all time steps is that the relative error of successive iterates should be less than 10^{-3}. These comparisons suggest that the algorithms perform better with large relaxation parameter α, which is predicted by the convergence analysis. It is also interesting to note that for a fixed α the number of iterations required at different time steps varies significantly. We believe that this is caused mainly by the fact that the solution varies significantly at different time steps.

References

[CF99]P. Cummings and X. Feng. Domain decomposition methods for a system of coupled acoustic and elastic Helmholtz equations. In C-H. Lai, P. Bjørstad, M. Cross, and O Widlund, editors, *Eleventh International Conference on Domain Decomposition Methods*, pages 203–210, Bergen, Norway, 1999. Domain Decomposition Press.

[CS76]A. Craggs and G. Stead. Sound transmission between enclosures - a study using plate and acoustic finite elements. *Acustica*, 35:89–98, 1976.

[Fen98]X. Feng. Interface conditions and non-overlapping domain decomposition methods for a fluid-solid interface problem. In J. Mandel, C. Farhat, and X.-C. Cai, editors, *Tenth International Conference on Domain Decomposition Methods*, pages 417–424. AMS, Contemporary Mathematics 218, 1998.

[QPV92]A. Quarteroni, F. Pasquarelli, and A. Valli. Heterogeneous domain decomposition principles, algorithms, applications. In David E. Keyes, Tony F. Chan, Gérard A. Meurant, Jeffrey S. Scroggs, and Robert G. Voigt, editors, *Fifth International Symposium on Domain Decomposition Methods for Partial Differential Equations*, pages 129–150, Philadelphia, PA, 1992. SIAM.

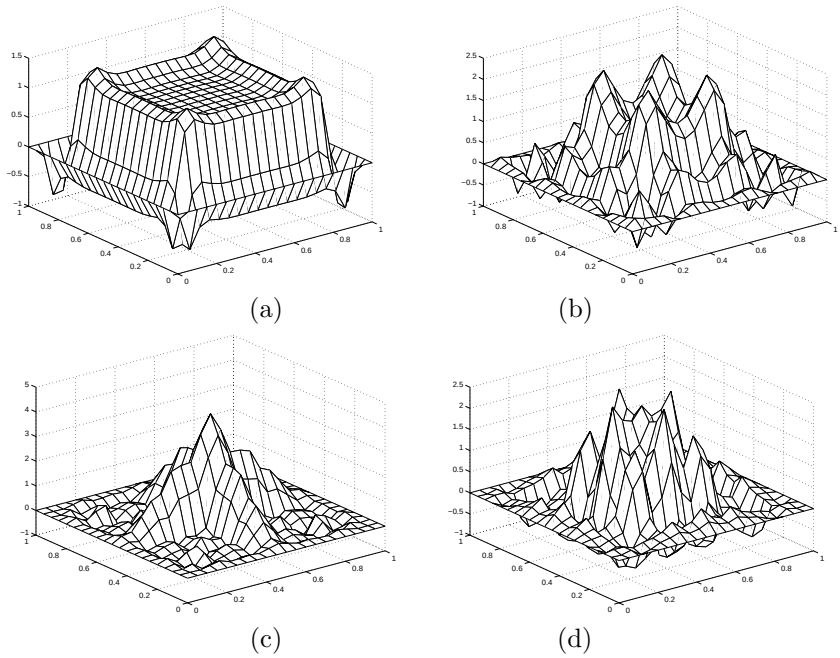

Figure 1: *Plate displacement profiles at different time steps*

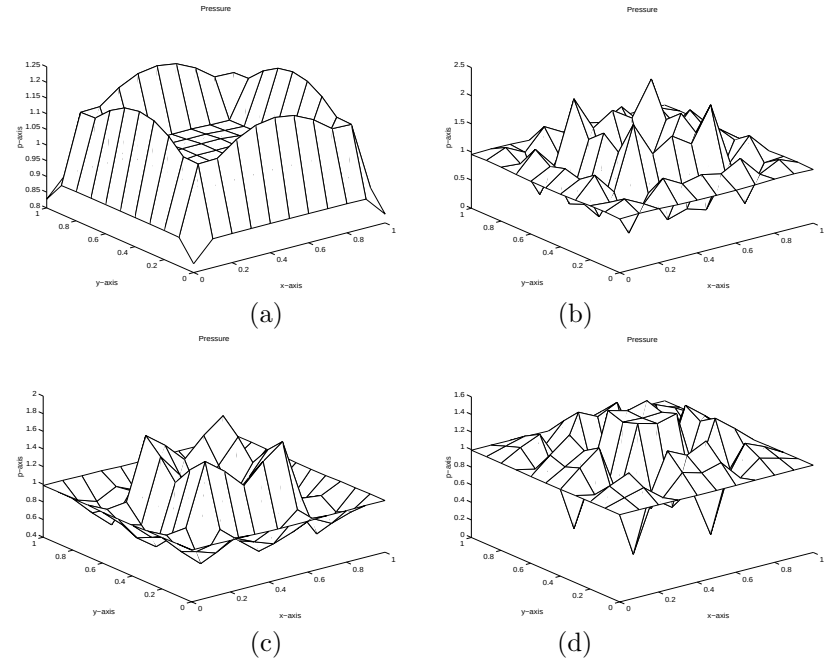

Figure 2: *Pressure profiles on the interface at different time steps*

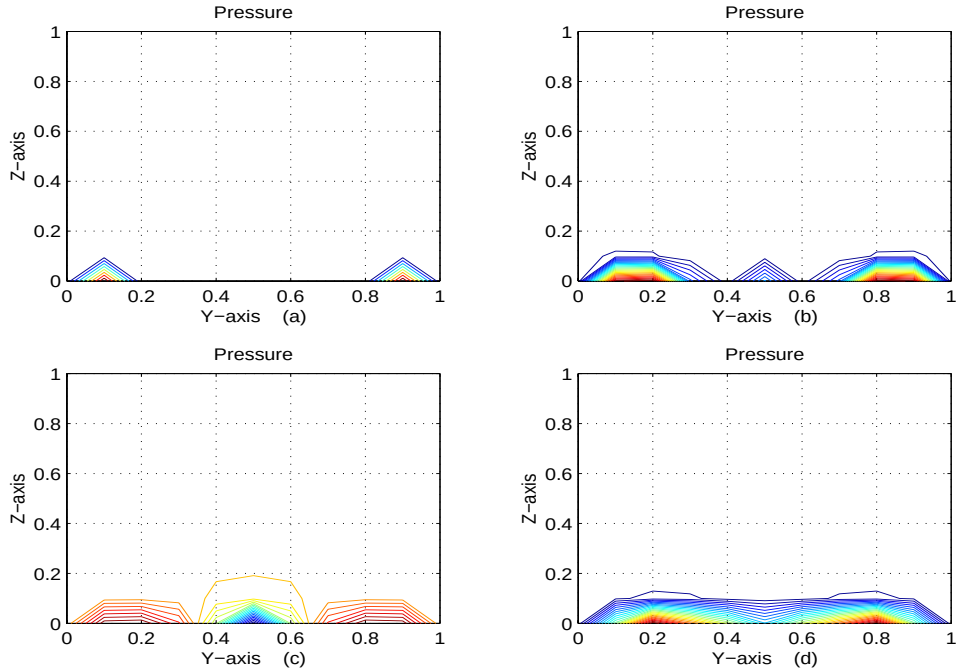

Figure 3: *Contour plots of the pressure p on the cross section $x_1 = 2$ at different time steps*

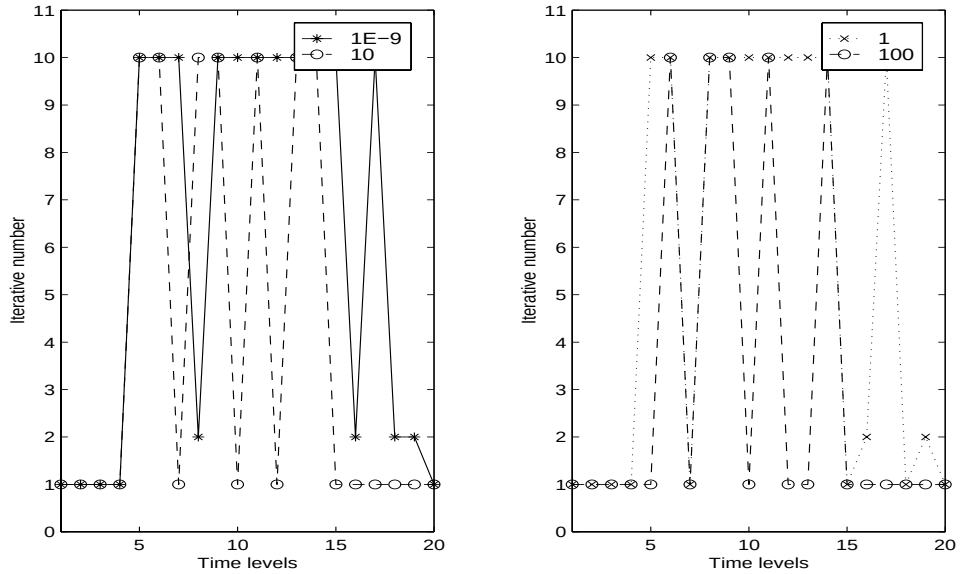

(a) (b)

Figure 4: Comparison of the iteration numbers for different value α at various time steps